Acta Chim. Slov. **2010,** *57,* 507–512

Scientific paper

Patterns of Ring Current in Coronene Isomers

Alexandru T. Balaban,[1,]* David E. Bean[2] and Patrick W. Fowler[2]

[1] Texas A&M University at Galveston, 5007 Avenue U, Galveston, Texas 77551, USA

[2] Department of Chemistry, University of Sheffield, S3 7HF, UK

** Corresponding author: E-mail: balabana@tamug.edu*

Received: 01-02-2010

This paper is dedicated to Professor Milan Randić on the occasion of his 80th birthday

Abstract

The ipsocentric pseudo-π model is used to predict maps of induced current density for isomeric variations of coronene in which the central hexagonal ring is surrounded by 5, 6, and 7-membered rings. All isomers in the set are predicted to support strong diatropic perimeter ring currents, thereby conforming to the magnetic criterion of aromaticity.

Keywords: Coronene isomers; ring currents; diatropic perimeter currents; local aromaticity

1. Introduction

Calculations of ring currents[1] have a long history, and in 1962 two independent calculations for coronene gave results that were in agreement. [2] It has been reported that in an axial magnetic field, a number of annular molecules such as coronene,[3] corannulene ([5]circulene[3]), [7]circulene[4] and kekulene[5] all support disjoint counter-rotating ring currents with the periphery having a diatropic ring current and the hub a paratropic ring current. By contrast, [10,5]coronene with ten fused pentagons around a central decagon was found to support inverted counter-rotating paratropic-rim versus diatropic-hub ring currents.[6] A similar pattern was found for the hypothetical corazulene molecule.[7] This sensitivity of current maps to changes in arrangements within polycycles is of course of interest in view of the connection between induced current and one popular definition of aromaticity, in which the defining characteristic of an aromatic cycle is that it should sustain a diatropic ring current.[8] This association of aromaticity and magnetic properties has been subject to much discussion over the years.[9]

A case of strong diatropic peripheral ring current which lacks opposition from the ring current in the hub was discovered for a valence isomer of coronene (which will be called here '[575757]isocoronene' for short)[10] having alternate heptagons and pentagons surrounding a central benzenoid ring. One may view this valence isomer as arising from the replacement of three naphthalenic units by azulenic subgraphs on the coronene periphery, without drastic reduction of aromaticity.

It is easy to imagine a gradual transition from coronene to this valence isomer, replacing stepwise a pair of peripheral hexagons of coronene by a pentagon and a heptagon in various positions around the central hexagon. One may also conceive more drastic changes corresponding to replacement of non-adjacent pairs of hexagonal rings, which may lead to adjacent pentagons and/or heptagons. Lower aromaticity will be associated with the presence of two adjacent five-membered rings (introducing an 8-circuit subgraph) or two adjacent seven-membered rings (forming a 12-circuit). Of course, the geometry of the valence isomers involving deviations from planarity must be taken into consideration.

The theoretical approach used here for the assessment of these progressive changes in aromaticity, at least in so far as this is determined by the presence of diatropic ring currents, involves the ipsocentric[11] (CTOCD-DZ)[12,13] method. Figure 1 shows the 18 isomers considered. They represent possible stages in a stepwise transition from coronene (**1**) to [575757]isocoronene (**18**). To begin with, two of the hexagons around the central benzenoid ring are replaced by one heptagon and one pentagon in all possible ways to give the para (**2**), ortho (**3**), and meta (**4**) configurations. In the next step, the central ring is surrounded by two pentagons, two hexagons, and two heptagons. The 11 possible configurations are represented in isomers

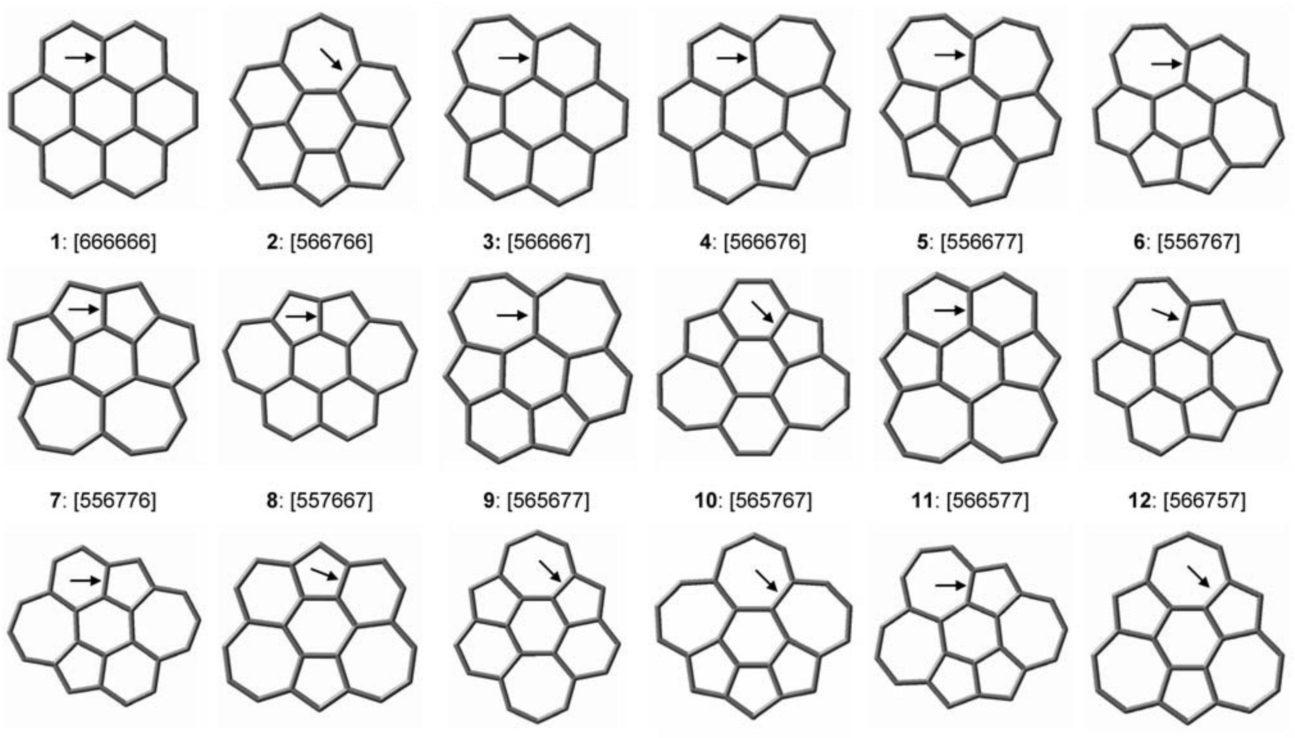

1: [666666] **2**: [566766] **3**: [566667] **4**: [566676] **5**: [556677] **6**: [556767]

7: [556776] **8**: [557667] **9**: [565677] **10**: [565767] **11**: [566577] **12**: [566757]

13: [567567] **14**: [567576] **15**: [567657] **16**: [555777] **17**: [557577] **18**: [575757]

Figure 1. The 18 ring-replacement isomers of coronene (**1**) studied here. This figure shows skeleton geometries optimized at maximum symmetry at the B3LYP/6-31G** level. No particular bonding scheme is implied. At this level, **7** and **16** are transition states. The arrows on the figure are referred to later in the text.

5–15. Isomers **16–18** show the three ways of arranging three heptagons and three pentagons around the central hexagon. Each isomer has a six-figure code which details the cyclic sequence of pentagons, hexagons and heptagons around the benzenoid centre. Several of these systems were considered in the early work of Randić and Trinajstić on conjugation and aromaticity in corannulenes, which concluded that many of them were aromatic in character.[14]

2. Method

All geometries are optimized at the B3LYP/6-31G** and RHF/6-31G** levels using Gaussian 09.[15] In the first instance, all structures are constrained to their maximum symmetries and optimized using both methods. Any structures found to be transition states or higher stationary points are then re-optimized without symmetry constraints to find the minimum geometry.

Ring currents are calculated using the well-established ipsocentric CTOCD-DZ approach at the CHF (Coupled Hartree-Fock) level.[11–13] Rather than completing full *ab initio* calculations for each structure, the pseudo-π approximation is used,[16] where each carbon atom is replaced with a hydrogen atom bearing a single 1s (STO-3G) orbital. This method relies on the one-to-one correspondence between the π orbitals of a planar conjugated system and the σ orbitals of the hydrogen cluster.

There is an astonishingly good numerical match between the σ current density of the hydrogen framework plotted in the molecular plane and the π current density of the original carbon system plotted at a height of $1a_0$. The pseudo-π method provides an economical way of reproducing the features of a ring current, and has already been successfully used on large polycyclic aromatic hydrocarbons.[17] Pseudo-π current-density maps for **1** and **18** in this paper compare well with *ab initio* π maps calculated elsewhere.[18]

The pseudo-π current-density maps are plotting using a combination of GAMESS-UK[19] and SYSMO[20] as implemented by Dr. R. W. A. Havenith. In the maps, anticlockwise (clockwise) circulation represents an induced diatropic/aromatic (paratropic/antiaromatic) current.

3. Results and Discussion

The maximum symmetries of **1–18**, along with the point group of their geometric minima at both the RHF and DFT levels, are given in Table 1. The table shows how unconstrained DFT optimization of these isomers often yields a structure with higher symmetry than the equivalent RHF result. Situations in which Hartree-Fock geometry optimization gives a lower symmetry than expected from the molecular graph are not uncommon, but DFT optimization tends to restore the higher symmetry, suggesting that the HF symmetry breaking is spurious.[21] It is often said that DFT optimization tends to favour more 'delocalised' systems,[22] and this is illustrated in the present series by reduced bond alternation compared to the RHF-optimized structures.

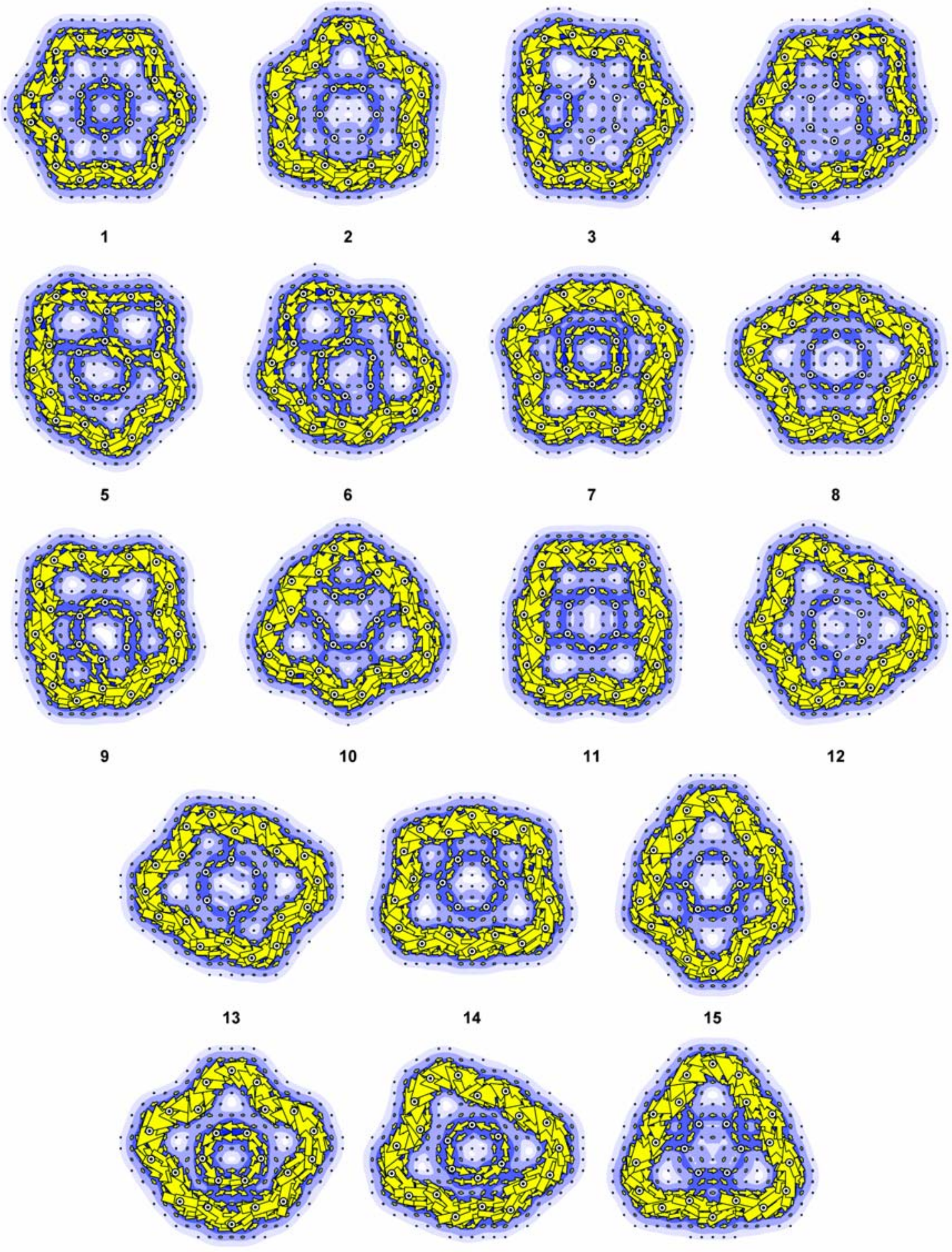

1 2 3 4 5 6 7 8 9 10 11 12 13 14 15 16 17 18

Figure 2. Pseudo-π current-density maps, calculated using the maximum-symmetry B3LYP/6-31G** geometries of isomers **1**–**18**.

Table 1. The maximum symmetry of each isomer (G_{max}) and the symmetries of its geometric minima (G_{min}) at the DFT/RHF levels are shown, along with the number of Kekulé structures. The Pauling Bond Order of each of the six 'spokes' bonds is given, beginning with the spoke highlighted by an arrow in Figure 1, and continuing in a clockwise direction around the central hexagon.

	G_{max}	G_{min}	Number of Kekulé Structures	Pauling Bond Order of the 'spokes' (total)
1	D_{6h}	D_{6h} /D_{6h}	20	0.40, 0.40, 0.40, 0.40, 0.40, 0.40 (2.40)
2	C_{2v}	C_{2v} /C_s	8	0.13, 0.25, 0.13, 0.13, 0.25, 0.13 (1.02)
3	C_s	C_s/C_s	12	0.25, 0.42, 0.33, 0.42, 0.25, 0.00 (1.67)
4	C_s	C_s/C_s	10	0.30, 0.10, 0.10, 0.30, 0.30, 0.30 (1.40)
5	C_s	C_s/C_s	7	0.14, 0.00, 0.14, 0.00, 0.14, 0.43 (0.85)
6	C_s	C_s/C_s	8	0.25, 0.13, 0.13, 0.13, 0.13, 0.25 (1.02)
7	C_{2v}	C_s /C_1	9	0.11, 0.22, 0.22, 0.11, 0.22, 0.22 (1.10)
8	C_{2v}	C_{2v}/ C_s	7	0.14, 0.00, 0.14, 0.43, 0.14, 0.00 (0.85)
9	C_s	C_s/C_s	8	0.13, 0.13, 0.25, 0.25, 0.13, 0.13 (1.02)
10	C_{2v}	C_{2v}/C_{2v}	9	0.22, 0.11, 0.22, 0.22, 0.11, 0.22 (1.10)
11	C_{2v}	C_{2v}/C_s	7	0.43, 0.14, 0.00, 0.14, 0.00, 0.14 (0.85)
12	C_s	C_s/C_s	7	0.00, 0.14, 0.00, 0.14, 0.43, 0.14 (0.85)
13	C_{2h}	C_{2h}/C_s	9	0.22, 0.11, 0.22, 0.22, 0.11, 0.22 (1.10)
14	C_{2v}	C_{2v}/C_s	8	0.25, 0.13, 0.13, 0.13, 0.13, 0.25 (1.02)
15	C_{2v}	C_{2v}/C_s	8	0.13, 0.13, 0.25, 0.25, 0.13, 0.13 (1.02)
16	C_{2v}	C_s/C_1	4	0.00, 0.00, 0.00, 0.00, 0.00, 0.00 (0.00)
17	C_s	C_s/C_s	4	0.00, 0.00, 0.00, 0.00, 0.00, 0.00 (0.00)
18	D_{3h}	D_{3h} /C_{3h}	4	0.00, 0.00, 0.00, 0.00, 0.00, 0.00 (0.00)

A recent study[23] of current-density maps for DFT and RHF geometries of polycyclic systems concluded that calculated ring current can be affected significantly by choice of geometry and use of a DFT optimized geometry was recommended. To provide consistent results across the range of isomers considered here, DFT geometries are used to plot the ring currents displayed in this paper.

Not every polycyclic system can achieve the theoretical maximum symmetry consistent with the graph of its carbon framework. Here, isomers **7** and **16** have geometric minima at the DFT level with lower than the maximum possible symmetry. In these isomers, adjacent pentagons and heptagons around the perimeter apparently cause sufficient strain to force the system to relax into a non-planar conformation.

Figure 2 shows the pseudo-π current-density maps plotted using the symmetry-constrained geometries, optimized at the B3LYP/6-31G** level. The isomers all show a strong diatropic perimeter current. Less intense currents are also apparent in the molecular interior, and in some cases (e.g. **7**, **16**, and **17**), this amounts to a marked diatropic circulation on the central hexagon. Apart from coronene (**1**) itself, none of the isomers show a diatropic-rim/paratropic-hub pattern.

Figure 3 shows the low-symmetry geometries of isomers **7** and **16** and their pseudo-π current-density maps. For these non-planar isomers the maps are plotted in the median plane and show the projection of current into that plane. Both molecules retain the diatropic perimeter currents seen in Figure 2, although here these are made harder to see by the undulation of the carbon framework with respect to the plotting plane. Relaxation of symmetry does not disrupt the rim-and-hub pattern of ring currents significantly.

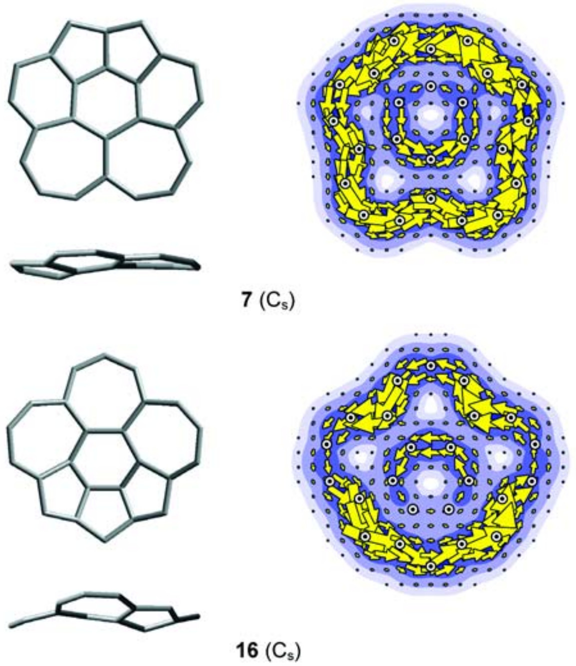

7 (C_s)

16 (C_s)

Figure 3. The structures and current-density maps for the unconstrained B3LYP/6-31G** optimizations of **7** and **16**. Sideways-on views (from the left) indicate the extent of deviation from planarity.

One model often used when discussing currents in circulene-type molecules is the "annulene-within-an-annulene" model (AWA).[24] In this model the perimeter and hub are be considered as separate cycles with their own electron counts, each subject separately to the Hückel 4*n*

+ 2 rule. In the limit where the cycles are non-interacting, this picture of the electronic structure leads to the prediction of con-rotating diatropic rim-and-hub currents for systems where both cycles achieve the aromatic electron count. Where the coupling between rim and hub cycles is strong, a simple Hückel-London treatment[25] predicts that the central hub current will be reversed, giving a counter-rotating system.

In this connection, our maps for **7**, **16** and **17** conform to the classic AWA prediction. On the other hand, as has already been noted,[26] the central paratropic current in coronene (**1**) can be reconciled with the AWA model only if it is assumed that there is strong coupling between perimeter and hub. Most of the remaining maps fall into the crossover region where the central current is weak, which would be characteristic of intermediate coupling strengths.[25,27] Some support for this interpretation of the pseudo-π maps comes from consideration of Kekulé structures and Pauling bond orders. The Pauling bond order (PBO) of a C-C bond in a Kekulean hydrocarbon is the fraction of molecular Kekulé structures in which that bond is formally double. As Table 1 shows, the 'spoke' bonds in **16** and **17** all have PBO = 0 whereas the total PBO for the spoke bonds in **1** is 2.4, the largest sum within the isomer set. The correlation with the computed maps is clearly not perfect, however, as for example isomer **18** has six spokes with PBO=0 but no concerted hub current.

The ring replacement strategy described in the introduction can be taken further, replacing the outer hexagons of coronene with squares and octagons, rather than pentagons and heptagons. At the B3LYP/6-31G** level of optimisation, the [484848] arrangement has a non-planar C_{3v} structure, and the pseudo-π current map displays con-rotating paratropic hub and perimeter circulations. Figure 4 shows the map for the maximum symmetry D_{3h} transition state, which has essentially the same pattern as the stacked currents of the C_{3v} structure, even if probably overestimated in this model owing to the small HOMO-LUMO gap; the D_{3h} map has the advantage that it can be viewed on a single current-density plot.

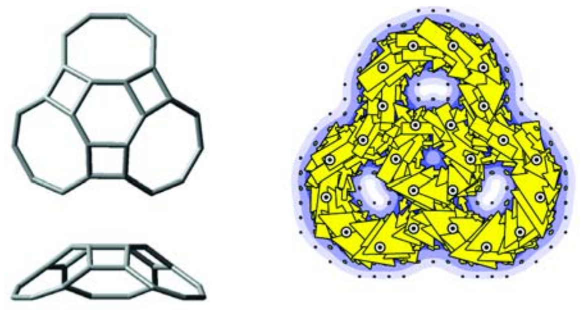
[484848] (C_{3v} structure) [484848] (D_{3h} map)

Figure 4. The structure of the C_{3v} geometric minima of [484848] (top-down and side-on views), and the pseudo-π current calculated using a D_{3h}-constrained geometry.

4. Conclusion

The observation that all isomers **1–18** support strong diatropic perimeter currents corresponds to a prediction of (magnetic) aromaticity for all these species, which would be reflected in the chemical shifts of exo-protons, for example. Starting with Polansky and Derflinger's paper,[28] some theoretical chemists have also argued that one can compute local aromaticities or antiaromaticities for individual rings of polycyclic conjugated compounds. On the other hand, the difficulties that plague the precise definition of global aromaticity are magnified for local aromaticities.[29] Progress in reconciling, for example, NICS[30] values for individual rings and current-density maps in polycyclic aromatic hydrocarbons (PAH) has been made using multicentre delocalisation indices.[31,32] A direct qualitative insight into the partitioning of π-electrons between rings is given by the Randić-Balaban model,[33,34,35,36] which is based on Kekulé structures, and has shown good correlations with ring current for some classes of PAH, but has difficulties with coronene-like systems. For coronene, relative ring currents[37] do not correlate well with π-electron partitions, as recently discussed.[38]

What is clear from our model calculations for isomers **1–18** is that the coronene structure shows considerable tolerance of variation in ring size and placement. All 18 isomers have an equal claim to the label 'aromatic' (on the ring current criterion) in spite of their likely differences in stability and reactivity.

5. Reference

1. See for example: P. Lazzeretti, *Prog. Nuc. Mag. Res. Sp.* **2000**, *36*, 1–88.
2. See for example: (a) I. J. Maddox, R. McWeeny, *J. Chem. Phys.* **1962**, *36*, 2353–2354. (b) N. Jonathan, S. Gordon, B. P. Dailey, *J. Chem. Phys.* **1962**, *36*, 2443–2448.
3. E. Steiner, P. W. Fowler, L. W. Jenneskens, *Angew. Chem. Int. Ed.* **2001**, *40*, 362–366.
4. A. Acocella, R. W. A. Havenith, E. Steiner, P. W. Fowler, L. W. Jenneskens, *Chem. Phys. Lett.* **2002**, *363*, 64–72.
5. E. Steiner, P. W. Fowler, L. W. Jenneskens, A. Acocella, *Chem. Comm.* **2001**, 659–660.
6. G. Monaco, R. G. Viglione, R. Zanasi, P. W. Fowler, *J. Phys. Chem. A* **2006**, *110*, 7447–7452.
7. M. Lillington, P. W. Fowler, M. V. Diudea, *Polish J. Chem.* **2007**, *81*, 653–662.
8. (a) J. A. Elvidge, L. M. Jackman, *J. Chem. Soc.* **1961**, 859–866. (b) J. A. Elvidge, *Chem. Commun.* **1965**, 160–161. (c) P. v. R. Schleyer, H. Jiao, *Pure Appl. Chem.* **1996**, *68*, 209–218.
9. See for example: (a) A. T. Balaban, *Pure Appl. Chem.* **1980**, *52*, 1409–1429. (b) R. B. Mallion, *Pure. Appl. Chem.* **1980**, *52*, 1541–1548. (c) J. A. N. F. Gomes, R. B. Mallion, *Chem. Rev.* **2001**, *101*, 1349–1383.

10. A. Ciesielski, M. K. Cyrañski, T. M. Krygowski, P. W. Fowler, M. Lillington, *J. Org. Chem.* **2006**, *71*, 6840–6845.
11. E. Steiner, P. W. Fowler, *J. Phys. Chem. A* **2001**, *105*, 9553–9562.
12. T. A. Keith, R. F. W. Bader, *Chem. Phys. Lett.* **1993**, *210*, 223–231.
13. S. Coriani, P. Lazzeretti, M. Malagoli, R. Zanasi, *Theor. Chim. Acta.* **1994**, *89*, 181–192.
14. M. Randić, N. Trinajstić, *J. Am. Chem. Soc.* **1984**, *106*, 4428–4434.
15. Gaussian 09, Revision A.02, M. J. Frisch, G. W. Trucks, H. B. Schlegel, G. E. Scuseria, M. A. Robb, J. R. Cheeseman, G. Scalmani, V. Barone, B. Mennucci, G. A. Petersson, H. Nakatsuji, M. Caricato, X. Li, H. P. Hratchian, A. F. Izmaylov, J. Bloino, G. Zheng, J. L. Sonnenberg, M. Hada, M. Ehara, K. Toyota, R. Fukuda, J. Hasegawa, M. Ishida, T. Nakajima, Y. Honda, O. Kitao, H. Nakai, T. Vreven, J. A. Montgomery, Jr., J. E. Peralta, F. Ogliaro, M. Bearpark, J. J. Heyd, E. Brothers, K. N. Kudin, V. N. Staroverov, R. Kobayashi, J. Normand, K. Raghavachari, A. Rendell, J. C. Burant, S. S. Iyengar, J. Tomasi, M. Cossi, N. Rega, J. M. Millam, M. Klene, J. E. Knox, J. B. Cross, V. Bakken, C. Adamo, J. Jaramillo, R. Gomperts, R. E. Stratmann, O. Yazyev, A. J. Austin, R. Cammi, C. Pomelli, J. W. Ochterski, R. L. Martin, K. Morokuma, V. G. Zakrzewski, G. A. Voth, P. Salvador, J. J. Dannenberg, S. Dapprich, A. D. Daniels, O. Farkas, J. B. Foresman, J. V. Ortiz, J. Cioslowski, and D. J. Fox, Gaussian, Inc., Wallingford CT, **2009**.
16. P. W. Fowler, E. Steiner, *Chem. Phys. Lett.* **2002**, *364*, 259–266.
17. E. Steiner, P. W. Fowler, A. Soncini, L. W. Jenneskens, *Faraday Discuss.* **2007**, *135*, 309–323.
18. A. Ciesielski, M. K. Cyrañski, T. M. Krygowski, P. W. Fowler, M. Lillington, *J. Org. Chem.* **2006**, *71*, 6840–6845.
19. M. F. Guest, I. J. Bush, H. J. J. Van Dam, P. Sherwood, J. M. H. Thomas, J. H. Van Lenthe, R. W. A. Havenith, J. Kendrick, *Mol. Phys.* **2005**, *103*, 719–747.
20. P. Lazzeretti, R. Zanasi, SYSMO Package, University of Modena, **1980**. Additional routines by P. W. Fowler, E. Steiner, R. W. A. Havenith, A. Soncini.
21. C. D. Sherrill, M. S. Lee, M. Head-Gordon, *Chem. Phys. Lett.* **1999**, *302*, 425–430.
22. A. Soncini, P. W. Fowler, L. W. Jenneskens, *Phys. Chem. Chem. Phys.* **2004**, *6*, 277–284.
23. R. W. A. Havenith, A. J. H. M. Meijer, B. J. Irving, P. W. Fowler, *Mol. Phys.* **2009**, *107*, 2591–2600.
24. E.g. R. Benshafrut, E. Shabtai, M. Rabinovitz, L. T. Scott, *Eur. J. Org. Chem.* **2000**, 1091–1106.
25. E. Steiner, P.W. Fowler, L.W. Jenneskens, A. Acocella, *Chem. Comm.* **2001***,* 659–660.
26. E. Steiner, P. W. Fowler, L. W. Jenneskens, *Angew. Chem. Int. Ed.* **2001**, *40*, 362–366.
27. G. Ege, H. Vogler, *Theor. Chim. Acta.* **1972**, *26*, 55–65.
28. O. Polansky, G. Derflinger, *Int. J. Quantum Chem.* **1967**, *1*, 379–401.
29. P. Bultinck, *Faraday Discuss.* **2007**, *135*, 347–365.
30. P. v. R. Schleyer, C. Maerker, A. Dransfeld, H. Jiao, N. J. R. van Eikema Hommes, *J. Am. Chem. Soc.* **1996**, *118*, 6317–6318.
31. S. Fias, S. van Damme, P. Bultinck, *J. Comput. Chem.* **2008**, *29*, 358–366.
32. S. Fias, P. W. Fowler, J. L. Delgado, U. Hahn, P. Bultinck, *Chem. Eur. J.* **2008**, *14*, 3093–3099.
33. M. Randić, A. T. Balaban, *Polycyclic Arom. Comp.* **2004**, *24*, 173–193.
34. A. T. Balaban, M. Randić, *New J. Chem.* **2004**, *28*, 800–806.
35. A. T. Balaban, M. Randić, *J. Math. Chem.* **2005**, *37*, 443–453.
36. A. T. Balaban, M. Randić, *New J. Chem.* **2008**, *32*, 1071–1078.
37. R. B. Mallion, *Croatica Chem. Acta* **2008**, *81*, 227–246.
38. A. T. Balaban, R. B. Mallion, submitted for publication.

Povzetek

Uporabili smo izocentrični psevdo-π model za napoved mape porazdelitve induciranega gostotnega toka za izomerne variacije koronena, v katerem je centralni šesterni obroč obkrožen s 5, 6 in 7-členskimi obroči. Vse napovedi za izomere študiranega niza podpirajo hipotezo močnih diatropičnih tokov perimetričnega obroča, kar ustreza magnetskemu kriteriju aromatičnosti.